PROPOSAL FOR A FILTERLESS FLUORESCENCE SENSOR FOR SNP GENOTYPING

K. Yamasaki[1], H. Nakazawa[1,2], N. Misawa[1,3], M. Ishida[1,3] and K. Sawada[1,3,4]
[1]*Toyohashi University of Technology (TUT), 1-1 Hibarigaoka, Tempaku-cho, Toyohashi, Aichi 441-8580, Japan*
[2]*JSPS Research Fellow, Chiyoda, Tokyo 102-8472, Japan*
[3]*Electronics-Inspired Interdisciplinary Research Institute (EIIRIS), Toyohashi, Aichi 441-8580, Japan*
[4]*JST-CREST, Chiyoda, Tokyo 102-8666, Japan*

Keywords: SNP genotyping, Fluorescence, Filterless, Multiwavelength.

Abstract: This study describes a biosensor for single nucleotide polymorphism (SNP) genotyping based on the filterless fluorescence detection methods. The filterless fluorescence sensor is able to distinguish lights with more than two different wavelengths without optical filters, mirrors, and gratings. From the final results, we observed that emission lights form the "fluorescein isothiocyanate (i.e., FITC)" and the "sulforhodamine 101 acid chloride (i.e., Texas Red)", which are kinds of fluorescent dyes commonly used in SNP genotyping, were detected with less interference using the filterless fluorescence sensor. Thus, our approach is effective for SNP genotyping with low cost and high portability.

1 INTRODUCTION

Micro-total analysis systems (μ-TAS) are highly desirable for the detection of various types of biochemical information with low cost and high portability. Furthermore, μ-TAS offers the potential for highly efficient, simultaneous analysis of a large number of biologically important molecules in genomic, proteomic and metabolic studies.

μ-TAS compounds pumps, valves, reactors, heaters, micro-fluidic channels, and sensors. The various types of sensors that have functionality for biochemical analyses have recently been studied, with research aimed at compounding with μ-TAS.

One of the most useful sensing methods in biochemistry is the fluorescence detection method. We have previously devised a filterless fluorescence sensor which can be applied to the detection of fluorescence (Maruyama et al., 2006); (Maruyama et al., 2006); (Nakazawa et al., 2011). This sensor detected several signals with different wavelengths simultaneously, without the need for optical filters, mirrors, and gratings. In this paper, we purpose an ability of a filterless fluorescence sensor to apply to single nucleotide polymorphism (SNP) genotyping based on the filterless fluorescence detection method.

2 FILTERLESS FLUORESCENCE SENSOR

2.1 Sensor Structure

Figure 1 shows a photomicrograph of the devised sensor. The devised sensor was fabricated in our laboratory using 5-μm-rule, N-substrate, 1P1M (1-poly and 1-metal), and single well modified complementary metal-oxide semiconductor fabrication technology. The size of the sensing area is 300 × 300 μm^2, and the depth of the p-n junction is about 4 μm beneath the sensing area.

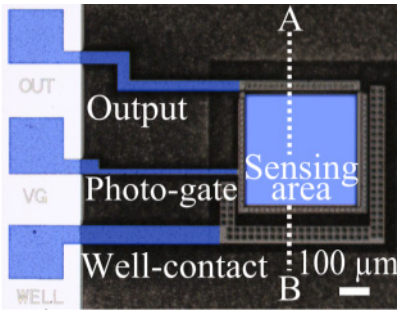

Figure 1: Photomicrograph of the fabricated filterless fluorescence sensor.

Yamasaki K., Nakazawa H., Misawa N., Ishida M. and Sawada K..
PROPOSAL FOR A FILTERLESS FLUORESCENCE SENSOR FOR SNP GENOTYPING.
DOI: 10.5220/0003774201850189
In *Proceedings of the International Conference on Biomedical Electronics and Devices* (BIODEVICES-2012), pages 185-189
ISBN: 978-989-8425-91-1

Figure 2 shows the concept and configuration of the devised sensor. The devised sensor is based on a photo-gate structure. The sensing area of the device consists of four layers: n-type poly-Silicon (500 nm)/SiO_2 (90 nm)/p-well (4 µm)/n-type silicon substrate.

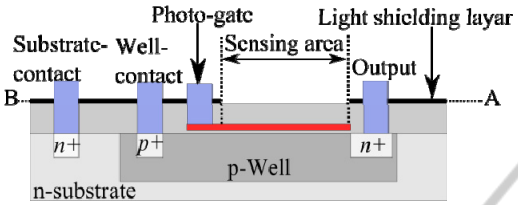

Figure 2: Schematic diagram of section A-B shown in Fig. 1. The cross-section structure is based on a photo-gate structure.

2.2 Basic Principle

The principle of the filterless fluorescence detection is based on the variation of optical absorption depth with wavelength (Mckelvey, 1996). When lights with two different wavelengths (e.g., fluorescence and the excitation light) are incident simultaneously, the currents I generated at absorption depths w_1 and w_2 are given by the following equations (1):

$$I_1=\frac{qS}{hc}\lambda_1\varphi_1(1-e^{-\alpha_1 w_1})+\frac{qS}{hc}\lambda_2\varphi_2(1-e^{-\alpha_2 w_1}),$$
$$I_2=\frac{qS}{hc}\lambda_1\varphi_1(1-e^{-\alpha_1 w_2})+\frac{qS}{hc}\lambda_2\varphi_2(1-e^{-\alpha_2 w_2}). \quad (1)$$

where φ_1 and φ_2 are the intensities at wavelengths λ_1 and λ_2 with absorption coefficients α_1 and α_2, respectively, S is the size of the sensing region, q is the elementary charge, h is the Planck constant, and c is the speed of light in a vacuum. Both illumination intensities (φ_1 and φ_2) are obtained by solving these simultaneous equations.

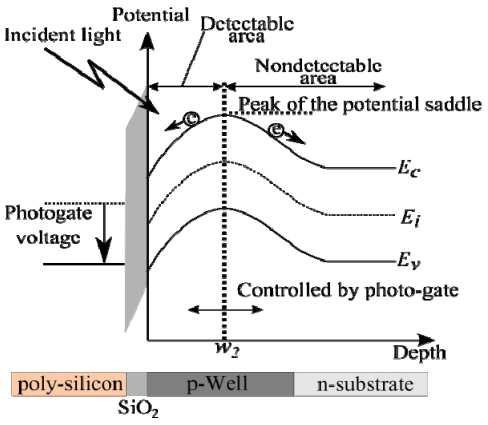

Figure 3: Potential distribution beneath the sensing area.

The energy band structure beneath the sensing region shown in Fig. 3 is essential for fluorescence sensing. A potential well is formed at the surface of the silicon substrate beneath the sensing region. The most important consideration for fluorescence sensing with the devised sensor is that the absorption depth w is tunable, because there is a variation in the absorption depth w for different wavelengths. In the devised sensor, the absorption depth w can be controlled by changing the photo-gate voltage, and electrons generated within the selected absorption depth w are collected for read out.

2.3 Sensing Procedure

Figure 4 shows a potential diagram for the intensity measurements of fluorescence and excitation light. If the photo-gate voltage is set to V_1 then the absorption depth changes to w_1. When light is incident on the sensing area, photons are absorbed in the depletion layer below the sensing area. Finally, the currents, I_1, generated at absorption depth w_1 are read out via the output node. The currents, I_2, generated at absorption depth w_2 are similarly obtained by changing the photo-gate voltage from V_1 to V_2.

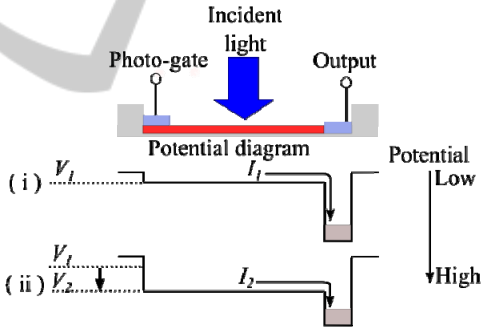

Figure 4: Potential diagram for the intensity measurements of fluorescence and excitation light.

3 EXPERIMENTS

3.1 Sensor Property

3.1.1 Wavelength Dependency

We investigated output current of the devised sensor for several wavelengths. The sensor was exposed to a range of wavelength lights from approx. 430 nm to 610 nm using programmable light source equipment (OSVIS-500, Tokyo Instruments, Inc.) in a dark room. Each power of the incident light was preliminarily measured using an external power meter

(8230E, ADC Corporation) to keep fixed light power of 100 μW/cm^2 for the reference.

3.1.2 Detection Limit

On the assumption of FITC use, the sensor was irradiated by commercial light emitting diode (LED) (L-7113VGC-H, Kingbright Elec. Co., Ltd.) that had the dominate wavelength of 525 nm and the output current was measured at 27 °C. Incident light power was changed from 0.1 to 100 μW/cm^2 confirmed by an external power meter (8230E, ADC Corporation).

3.1.3 Temperature Dependency

We investigated the influence of dark current which comes from thermal excitation. The surrounding temperature of the sensor was set 21, 27, and 35 °C independently. Then, output currents were measured.

3.2 Fluorescence Detection

3.2.1 Measurements of FITC and Texas Red

To confirm the sensor's performance of the quantitative measurements for fluorescent dyes, fluorescein isothiocyanate (FITC) and sulforhodamine 101 acid chloride (Texas Red) which are typically used bioanalysis including SNP genotyping, we measured the excited fluorescence intensity 525 nm of FITC (Wako Pure Chemical Industries, Ltd.) or 615 nm of Texas Red (Life Technologies Corporation) 200 μl solution of 0, 1, 10 μM individually. Each fluorescent solution was prepared using diluted ethanol (50v/v%). And the each sample solution was set in a cylindrical plastic chamber of a 7 mm inner diameter and a 10 mm height as shown in Fig. 5. The excitation lights, 490 nm and 590 nm, for FITC and Texas Red were independently applied by light source equipment (LAX-C100, Asahi Spectra Co., Ltd.).

The absorption depth of the sensor was varied by changing of photo-gate voltage. The intensity of the fluorescence light and excitation light can be calculated by using equations (1) where λ_1= 490 nm, α_1= 20.0×10^5 m^{-1}, w_1= 0.761 μm, and λ_2= 525 nm, α_2= 12.7×10^5 m^{-1}, w_2= 1.135 μm were substituted in the case of FITC use. In the same way, λ_1= 590 nm, α_1= 6.39×10^5 m^{-1}, w_1= 0.803 μm, and λ_2= 615 nm, α_2= 4.82×10^5 m^{-1}, w_2= 1.135 μm were substituted in the case of Texas Red use. The results of detected the light intensities were normalized assuming the intensity was 1.0 that was a value in the case of measuring 10 μM fluorescent solutions. Furthermore, we evaluated the possibilities of cross talks of two excitation lights, 590 nm and 490 nm, to FITC and Texas Red. Each fluorescent solution was additionally exposed by ineffective light for excitation (i.e., 590 nm light for FITC and 490 nm for Texas Red).

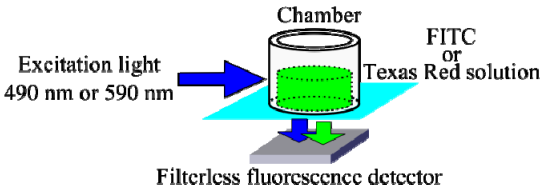

Figure 5: Schematic view of the measurement setup.

3.2.2 Detection of FITC and Texas Red Mix

As a model sample of a heterozygote in SNP variations, we additionally measured the 200 μl mixture solution of equal parts of FITC and Texas Red (net 0.5 μM for each). The results of detected light intensities were also normalized as same as above section experiment.

4 RESULTS AND DISCUSSION

Figure 6 shows that the correlation between wavelength and output current of the sensor. The result means that the sensor has high sensitivity near the center of 550 nm at least in this wavelength region. And also, the sensor has almost the same sensitivity level for emission wavelengths of FITC (525 nm) and Texas Red (615 nm).

We think that the similarity of the sensor's output current level of FITC and Texas Red will enable us to compare them without any other complicated calibrations in this study.

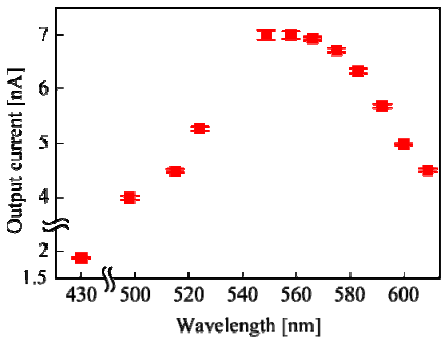

Figure 6: Wavelength dependency of the sensor's output.

Figure 7 shows the detection current versus the incident light intensity. Each data point was obtained by 10 times experiments and the each error bar was

standard deviation. Fig. 7(a) and (b) show the incident light intensity in the range of 2-100 μW/cm^2 and 0.1-2 μW/cm^2, respectively. The detection current is proportional to the incident light power in the range at least above about 0.1 μW/cm^2. The detection current was nearly equal to the dark current less than 0.1 μW/cm^2. This result implies that the sensor can almost linearly detect incident light in the range of 0.1-100 μW/cm^2.

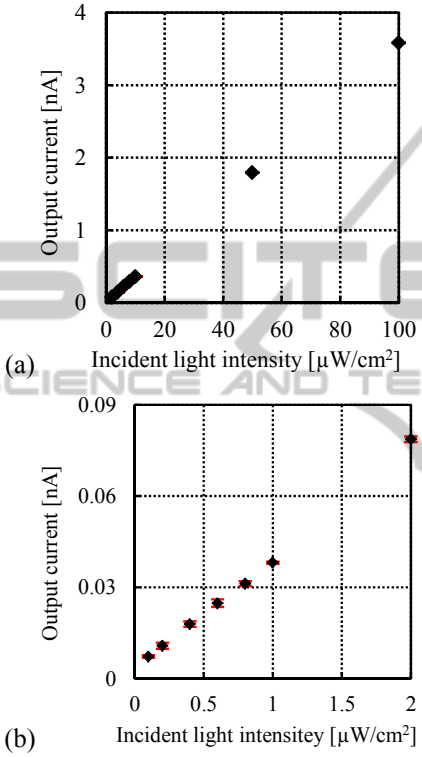

Figure 7: Detection current versus the incident light intensity in the range of 2-100 μW/cm^2 (a) and 0.1-2 μW/cm^2 (b).

Figure 8 shows the dark current level depending on the temperature. The result shows that dark current increases with increasing of surrounding temperature. According to the dark current level, we found that our sensor is able to detect the fluorescence intensity quantitatively in the range of more than about 0.1 μW/cm^2. And it is presumed that the dark current level is a few pA at room temperature.

The results of individual measurements of FITC and Texas Red solution are shown in Fig. 9. Each of them can be quantitatively detected in these rough differences in concentration. It implies that the sensor will be able to use for SNP genotyping because a typical concentration of polymerase chain reaction product is about 10 μM.

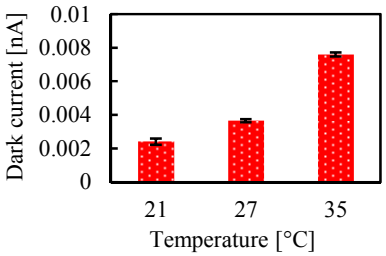

Figure 8: Temperature dependence of the dark currents of the devised sensor.

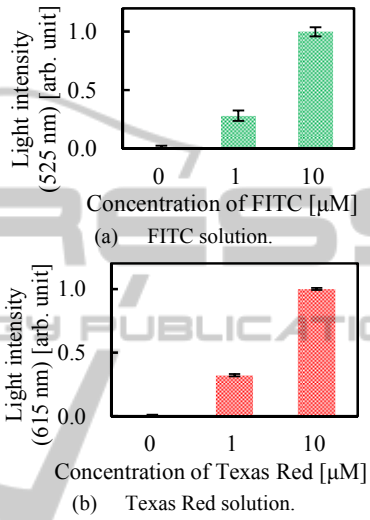

Figure 9: Concentration dependency of detected fluorescent intensities.

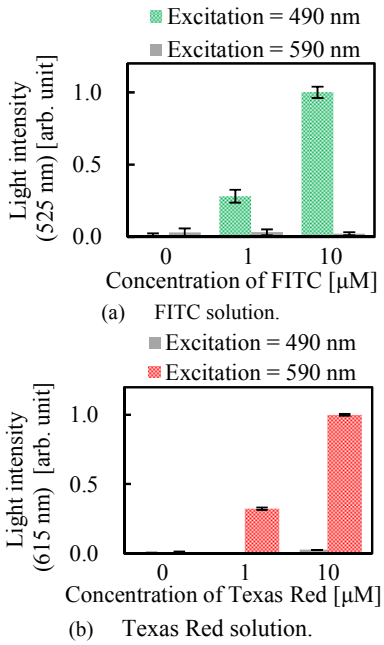

Figure 10: Differences of fluorescence intensity by the two different lights excitation.

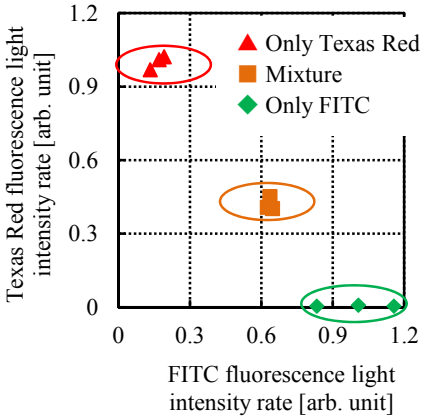

Figure 11: Distributions of fluorescence intensities for FITC solutions, Texas Red solutions and their mixtures.

Ideally, those mixtures should be measured to the center of both axes. However, they slightly leaned to FITC side. We suppose that this result comes from FITC appears large seemingly due to fluorescence of Texas Red which was excited by 490 nm light is mixed. According to these results, we think that the devised sensor could potentially be applied to real SNP genotyping for individual determination of homozygote or heterozygote.

5 CONCLUSIONS

We showed that our devised sensor could detect quantitatively fluorescent dyes; FITC and Texas Red without the filters. And, we found that the sensor successfully distinguished FITC and Texas Red solution and their mixture. We believe that the sensor enable us to SNP genotyping in compact system.

ACKNOWLEDGEMENTS

This work was partially supported by the Global COE Program titled Frontiers of Intelligent Sensing, the projects of the Hamamatsu Optoelectronics Knowledge Cluster Initiative, a grant-in-aid for scientific research (A) (No. 21246051) from the Ministry of Education, Culture, Sports, Science and Technology (MEXT) of Japan, and a grant-in-aid for JSPS Fellows from Japan Society for the Promotion of Science (JSPS).

REFERENCES

Y. Maruyama et al., IEEE Trans. Electron Devices, 53(3) (2006) 553–558.
Y. Maruyama et al., Sens. Actuators A 128 (2006) 66-70.
H. Nakazawa et al., Proc. Transducers 2011 (2011) 100-103.
J.P. Mckelvey, Solid State and Semiconductor Physics, Harper and Row, New York, 1966, p. 463.